

β -Amyloid PET and neuropathology in dementia with Lewy bodies

Kejal Kantarci, MD, MS, Val J. Lowe, MD, Qin Chen, MD, PhD, Scott A. Przybelski, BS, Timothy G. Lesnick, MS, Christopher G. Schwarz, PhD, Matthew L. Senjem, MS, Jeffrey L. Gunter, PhD, Clifford R. Jack, Jr., MD, Jonathan Graff-Radford, MD, David T. Jones, MD, David S. Knopman, MD, Neill Graff-Radford, MD, Tanis J. Ferman, PhD, Joseph E. Parisi, MD, Dennis W. Dickson, MD, Ronald C. Petersen, MD, PhD, Bradley F. Boeve, MD, and Melissa E. Murray, PhD

Correspondence

Dr. Kantarci
kantarci.kejal@mayo.edu

Neurology® 2020;94:e282-e291. doi:10.1212/WNL.0000000000008818

Abstract

Objective

β -Amyloid ($A\beta$) pathology is common in patients with probable dementia with Lewy bodies (DLB). However, the pathologic basis and the differential diagnostic performance of $A\beta$ PET are not established in DLB. Our objective was to investigate the pathologic correlates of ^{11}C -Pittsburgh compound B (PiB) uptake on PET in cases with antemortem diagnosis of probable DLB or Lewy body disease (LBD) at autopsy.

Methods

Autopsied cases who underwent antemortem PiB-PET and were assigned a clinical diagnosis of probable DLB or LBD at autopsy were included ($n = 39$). The primary endpoint was pathologic diagnosis of LBD, Alzheimer disease (AD), or mixed (LBD and AD) pathology; the secondary endpoints included Thal $A\beta$ phase and diffuse and neuritic $A\beta$ plaques.

Results

Lower global cortical PiB standardized uptake value ratio (SUVr) distinguished cases with LBD from cases with AD or mixed pathology with an accuracy of 93%. Greater global cortical PiB SUVr correlated with higher Thal $A\beta$ phase ($r = 0.75$, $p \leq 0.001$). Voxel-based analysis demonstrated that $A\beta$ pathology relatively spared the occipital lobes in cases with mixed pathology and LBD compared to cases with AD without LBD, in whom the entire cerebral cortex was involved. Global cortical PiB SUVr was associated primarily with the abundance of diffuse $A\beta$ plaques in cases with LBD in a multivariable regression model.

Conclusion

Lower PiB uptake accurately distinguishes cases with LBD from cases with AD or mixed pathology, correlating with the Thal $A\beta$ phase. The severity of diffuse $A\beta$ pathology is the primary contributor to elevated PiB uptake in LBD.

Classification of evidence

This study provides Class III evidence that lower PiB uptake accurately distinguishes patients with LBD from those with AD or mixed pathology.

RELATED ARTICLE

Editorial

Can amyloid PET differentiate “pure” LBD from AD with or without LBD copathology?

Page 103

MORE ONLINE

→ Class of Evidence

Criteria for rating therapeutic and diagnostic studies

[NPub.org/coe](https://www.ncbi.nlm.nih.gov/pmc/articles/PMC7288818/)

From the Departments of Radiology (K.K., V.J.L., Q.C., C.G.S., C.R.J.), Health Sciences Research (S.A.P., T.G.L.), Information Technology (M.L.S., J.L.G.), Neurology (J.G.-R., D.T.J., D.S.K., R.C.P., B.F.B.), and Laboratory Medicine and Pathology (J.E.P.), Mayo Clinic, Rochester, MN; Department of Neurology (Q.C.), West China Hospital, Chengdu, Sichuan; and Departments of Neurology (N.G.-R.), Psychiatry and Psychology (T.J.F.), and Laboratory Medicine and Pathology (D.W.D., M.E.M.), Mayo Clinic, Jacksonville, FL.

Go to [Neurology.org/N](https://www.neurology.org/N) for full disclosures. Funding information and disclosures deemed relevant by the authors, if any, are provided at the end of the article.

The Article Processing Charge was funded by Mayo Clinic.

This is an open access article distributed under the terms of the Creative Commons Attribution-NonCommercial-NoDerivatives License 4.0 (CC BY-NC-ND), which permits downloading and sharing the work provided it is properly cited. The work cannot be changed in any way or used commercially without permission from the journal.

GLOSSARY

A β = β -amyloid; **AD** = Alzheimer disease; **CAA** = cerebral amyloid angiopathy; **DLB** = dementia with Lewy bodies; **DP** = diffuse plaque; **LBD** = Lewy body disease; **MCALT** = Mayo Clinic Adult Lifespan Template; **MMSE** = Mini-Mental State Examination; **NFT** = neurofibrillary tangle; **NIA-AA** = National Institute on Aging–Alzheimer’s Association; **NP** = neuritic plaque; **pDLB** = probable DLB; **PiB** = ¹¹C-Pittsburgh compound B; **pRBD** = probable REM sleep behavior disorder; **SUVr** = standardized uptake value ratio.

Alzheimer disease (AD) pathology, particularly β -amyloid (A β) pathology, is common in patients with Lewy body disease (LBD) at autopsy.^{1–3} In keeping with that, more than half of the patients with probable dementia with Lewy bodies (pDLB) have elevated A β on PET scan.⁴ Investigation of the neuropathologic basis of A β PET findings in patients with pDLB or autopsy-confirmed LBD without AD is limited to single case studies or case series.^{5–8}

Neuritic plaques (NPs) comprised primarily of A β ₄₀ are a pathologic feature of AD and serve as the primary contributor to positive A β PET scans in cohorts with AD dementia.^{9–15} Diffuse plaques (DPs) comprised primarily of A β ₄₂ are common in normal aging, often occurring in the absence of neurofibrillary tangle (NFT)–tau pathology. DPs are typically abundant in patients with LBD.¹⁶ A subset of patients with LBD also have NPs with tau in the NP core, which are not readily distinguishable from DPs with A β PET and may lead to some inconsistencies in the determination of AD-related pathology in patients with pDLB.^{5,6,17,18} Understanding the pathologic basis of A β PET findings in LBD is critical for using A β PET as a biomarker of AD pathology in patients with pDLB and has particular relevance for the patient selection for clinical trials designed to target AD-related A β deposition.

One of the most widely investigated A β PET ligands is ¹¹C-Pittsburgh compound B (PiB). PiB-PET and autopsy correlation studies consistently indicate that PiB exclusively binds to the β -pleated sheet of the amyloid protein present in NP and DP in the cortical gray matter and the A β deposits in the vessel walls.^{10,17–19} Because the A β content varies across plaques and vascular deposits, PiB binding to DP and vascular deposits may be less prominent than to NP.¹⁷ Similar variations in ligand binding have also been observed with ¹⁸F-labeled A β PET ligands.^{9,13,15} Thus, there may be disagreement between the A β PET findings and neuropathologic diagnosis of AD in some patients with pDLB who have differential levels of DP and NP pathology.^{6,8}

In the current study, we investigated the pathologic basis of PiB-PET findings in clinically diagnosed patients with pDLB or cases who were found to have LBD at autopsy. Our objectives were (1) to determine the distribution of A β pathology and the optimal cutoff value to differentiate cases with AD or mixed AD and LBD pathology from cases with LBD with low or no AD pathology,²⁰ (2) to determine the

correlation of antemortem PiB-PET with the Thal A β phase at autopsy, and (3) to determine the contribution of NP and DP to PiB-PET findings in cases with LBD.

Methods

Participants

Participants of this study were from 2 longitudinal cohorts: the Mayo Clinic Alzheimer’s Disease Research Center and Mayo Clinic Study of Aging, which is a population-based cohort from Olmstead County, Minnesota.²¹ From these 2 cohorts, we studied participants who underwent antemortem PiB-PET imaging along with an MRI examination and autopsy at the Alzheimer’s Disease Research Center Neuropathology Core from 2006 to 2018 (n = 189), and we included participants diagnosed with pDLB according to 3rd Consortium Criteria²² at any time during their longitudinal clinical evaluation or who were diagnosed as having LBD at autopsy (n = 39). We used the 3rd rather than 4th Consortium Criteria for the clinical diagnosis of pDLB because all clinical evaluations occurred before the publication of the 4th Consortium Criteria.²⁰ Cases with additional AD or vascular disease pathology were not excluded. Clinical assessments were detailed in previous reports from these cohorts.^{21,23} Briefly, the presence of parkinsonism was determined from a Unified Parkinson’s Disease Rating Scale Part III score >4. Visual hallucinations were characterized by being fully formed, were not restricted to a single episode, and were not related to another medical issue, treatment, or advanced dementia. Fluctuations were considered to be present if the patient scored 3 to 4 on the 4-item Mayo Fluctuations Scale.²⁴ Probable REM sleep behavior disorder (pRBD) met the International Classification of Sleep Disorders-II diagnostic criteria B for pRBD.²⁵ The clinical assessments were performed without any access to PiB-PET results.

Pathologic examination

Standardized methods were used for the neuropathologic assessment by expert neuropathologists (M.E.M., D.W.D., and J.E.P.) blinded to PiB-PET results. Sampling was done according to the Consortium to Establish a Registry for Alzheimer’s Disease protocol²⁶ and the 4th Report of the DLB Consortium.²⁰ Lewy body pathology was immunohistochemically evaluated with the NACP antibody (1:3000, rabbit polyclonal; Mayo Clinic’s antibody) using a protocol (formic acid pretreatment and DAKO [Agilent Technologies, Santa Clara, CA] DAB polymer signal detection) that has been shown to be comparable to or better than other methods.²⁷

The presence, density, semiquantitative scores, and distribution of Lewy body–related pathology followed recommendations of the 4th Report of the DLB Consortium.²⁰ A β plaques and NFTs were evaluated with a modified Bielschowsky silver stain or thioflavin-S, as recommended by National Institute on Aging–Alzheimer’s Association (NIA-AA) criteria.^{28,29} As previously described,¹⁴ thioflavin-S microscopy was used to assign Thal amyloid phase.³⁰ The NP score was determined by a 4-point semiquantitative assessment: 0 = none, 1 = sparse, 2 = moderate, and 3 = frequent. A β immunohistochemistry in the neocortex, hippocampus, basal ganglia, and cerebellum was used to assign Thal amyloid phase as follows: phase 1 = neocortex, phase 2 = CA1/subiculum, phase 3 = basal ganglia or dentate fascia of the hippocampus, phase 4 = midbrain or CA4 of the hippocampus, and phase 5 = cerebellum. DPs were scored as 0 = none, 1 = sparse, 2 = moderate, or 3 = frequent, according to National Alzheimer Coordinating Center neuropathology guidelines.³¹ The distribution of NFT-tau pathology was used to assign a Braak NFT stage.³² We applied the label of AD only to cases who met the intermediate or high AD designations in the NIA-AA criteria.^{28,29}

Cases with intermediate- or high-likelihood DLB (according to the 4th Report of the DLB Consortium Criteria) who had low AD pathology (according to the NIA-AA criteria) were classified as LBD; cases with intermediate- or high-likelihood DLB and intermediate or high AD pathology were classified as having mixed LBD-AD pathology; and cases with intermediate or high AD and no LBD pathology or low-likelihood DLB were classified as having AD.

MRI and PiB-PET imaging

MRI examinations were performed at 3T (GE Healthcare, Chicago, IL). A 3D high-resolution magnetization-prepared rapid gradient echo acquisition with \approx 1-mm cubic resolution was obtained for anatomic segmentation and labeling. PET/CT scanners (GE Healthcare) operating in 3D mode were used to acquire PET images. Patients were injected with an average of 596 MBq (range 292–729 MBq) ¹¹C-PiB. After a 40-minute ¹¹C-PiB uptake period, a 20-minute PiB scan consisting of four 5-minute dynamic frames was obtained.

PiB-PET image analysis

PiB-PET image analysis was performed with an automated image processing pipeline, which included rigid registration of the PET image volumes to each subject’s own 3D T1-weighted MRI using SPM12. MRIs were segmented with Unified Segmentation in SPM12 with population-optimized priors and settings from the Mayo Clinic Adult Lifespan Template (MCALT). Regional cortical uptake of PiB was determined with the MCALT_ADIR122 atlas.³³ The global cortical PiB retention standardized uptake value ratio (SUVr) was obtained from the bilateral parietal (including posterior cingulate and precuneus), temporal, prefrontal, orbitofrontal, and anterior cingulate regions referenced to the cerebellar crus region as previously described.³⁴ PiB SUVr in each voxel was referenced to the median value of the right and left cerebellar crus uptake.

A voxel-based analysis was conducted in the MCALT space using SPM12 comparing PiB SUVr in the LBD group to those of both the mixed LBD-AD and AD groups. Maps of these comparisons were displayed at the $p < 0.05$ level. Correction for multiple comparisons was applied with false discovery rate error correction.

Statistical analysis

Characteristics of the subjects were described by means and SDs for continuous variables and counts and percentages for categorical variables. Differences in characteristics of the 3 groups were evaluated with 1-way analysis of variance or χ^2 tests. Contrasts were used with the analyses of variance to compare Mini-Mental State Examination (MMSE) scores for AD vs LBD and LBD-AD and for LBD-AD vs LBD. To compare global cortical PiB SUVr for LBD vs LBD-AD and AD, we calculated the area under the receiver operating curve, sensitivity, specificity, and accuracy. A Pearson correlation adjusted for time from MRI to death was used to describe and test for an association of Thal A β phase with global cortical PiB SUVr. We used a multiple linear regression model to examine whether NP, DP, or their interaction contributed to the global cortical PiB SUVr after adjusting for time from MRI to death.

Classification of evidence

The primary research question was to determine the distribution of A β pathology and the optimal cutoff value to differentiate cases with AD or mixed AD and LBD pathology from cases with LBD with low or no AD pathology. This study provides Class III evidence for distinguishing patients with LBD from those AD or mixed pathology using PiB SUVr.

Data availability

Anonymized data not published within this article will be made available by request from any qualified investigator.

Results

Clinical and pathologic characteristics of the cohort

Characteristics of the cohort classified by the pathologic group are listed in the table. The pathologic groups did not differ in age at imaging or death, time from imaging to death, *APOE* ϵ 4 status, or the Clinical Dementia Rating Sum of Boxes score at the time of imaging, but the frequency of women was higher in the LBD-AD (47%) group than in either the LBD (0%) or the AD (17%) group. Furthermore, the AD group on average had lower MMSE scores than the LBD or LBD-AD groups ($p < 0.01$). Whereas all cases in the LBD and AD groups had parkinsonism at the time of imaging, the frequency was lower in the LBD-AD (56%) group. Similarly, all cases in the LBD group had pRBD at the time of imaging, but frequencies were lower in the LBD-AD (69%) and AD (17%) groups. Visual hallucinations were observed more frequently in the LBD (77%) and LBD-AD (62%) groups than the AD (17%) group, but there were no differences in the frequency of fluctuations.

Table Demographic, clinical, and pathologic characteristics of the cohort^a

	LBD (n = 14)	LBD-AD (n = 19)	AD (n = 6)	Overall p value ^b
Age, y	73.8 (7.7)	72.6 (6.9)	69.3 (11.8)	0.53
Male, n (%)	14 (100)	10 (53)	5 (83)	0.008
APOE ε4, n (%)	6 (42.9)	13 (68.4)	5 (83.3)	0.16
Age at death, y	75.9 (8.0)	75.3 (6.9)	71.7 (13.1)	0.57
Time from imaging to death, y	2.0 (1.2)	2.8 (1.6)	2.5 (1.4)	0.37
MMSE score	21.1 (5.8)	16.9 (6.8)	7.0 (6.0)	<0.001
CDR Sum of Boxes score	6.8 (5.0)	8.3 (4.8)	9.8 (3.1)	0.41
Visual hallucinations, n (%)	10 (77)	10 (62)	1 (17)	0.043
Fluctuations, n (%)	10 (77)	10 (62)	3 (50)	0.48
Parkinsonism, n (%)	13 (100)	9 (56)	6 (100)	0.006
RBD, n (%)	13 (100)	11 (69)	1 (17)	<0.001
Clinical diagnosis, n (%)				
CN	1 (8)	1 (5)	0 (0)	<0.001
MCI	1 (8)	1 (5)	0 (0)	
pDLB	10 (77)	9 (47)	0 (0)	
pDLB and AD	1 (8)	1 (5)	6 (100)	
AD	0 (0)	7 (37)	0 (0)	
LBD pathology, n (%)				
None	0 (0)	0 (0)	4 (67)	<0.001
Amygdala only	0 (0)	0 (0)	2 (33)	
Transitional LBD	6 (43)	2 (11)	0 (0)	
Diffuse LBD	8 (57)	17 (89)	0 (0)	
NIA-AA level of AD pathology, n (%)				
Low	14 (100)	0 (0)	0 (0)	<0.001
Intermediate	0 (0)	12 (63)	0 (0)	
High	0 (0)	7 (37)	6 (100)	
Consortium pathologic diagnosis of DLB, n (%)				
Low likelihood DLB	0 (0)	0 (0)	6 (100)	<0.001
Intermediate-likelihood DLB	1 (7)	9 (47)	0 (0)	
High-likelihood DLB	13 (93)	10 (53)	0 (0)	
Braak NFT stage	2.0 (0.8)	4.4 (1.0)	5.7 (0.5)	<0.001
Thal Aβ phase	2.1 (1.6)	4.3 (0.9)	4.8 (0.4)	<0.001
Neuritic Aβ plaques, n (%)				
None	4 (29)	0 (0)	0 (0)	0.004
Sparse	7 (50)	5 (26)	0 (0)	
Moderate	3 (21)	5 (26)	2 (33)	
Frequent	0 (0)	9 (47)	4 (67)	

Continued

Table Demographic, clinical, and pathologic characteristics of the cohort^a (continued)

	LBD (n = 14)	LBD-AD (n = 19)	AD (n = 6)	Overall <i>p</i> value ^b
Diffuse Aβ plaques, n (%)				
None	4 (29)	0 (0)	0 (0)	0.002
Sparse	1 (7)	1 (5)	0 (0)	
Moderate	6 (43)	4 (21)	0 (0)	
Frequent	3 (21)	14 (74)	6 (100)	

Abbreviations: A β = β -amyloid; AD = Alzheimer disease; CDR = Clinical Dementia Rating; CN = cognitively normal; DLB = dementia with Lewy bodies; LBD = Lewy body disease; MCI = mild cognitive impairment; MMSE = Mini-Mental State Examination; NFT = neurofibrillary tangle; NIA-AA = National Institute on Aging–Alzheimer’s Association; pDLB = probable DLB; RBD = REM sleep behavior disorder

^a Pathologic group with the mean (SD) listed for the continuous variables and count (percent) for the categorical variables.

^b The *p* values for differences between groups come from an analysis of variance for the continuous variables or a χ^2 test for the categorical variables.

According to the clinical evaluation, there were cases with mild cognitive impairment ($n = 2$) and cognitively unimpaired cases both in the LBD group ($n = 2$) and in the LBD-AD group ($n = 2$). One of the cases with mild cognitive impairment had parkinsonism. All patients with a clinical diagnosis of pDLB had either LBD (10 of 19, 53%) or mixed LBD and AD pathology at autopsy (9 of 19, 47%). On the other hand, a majority of patients with a clinical diagnosis of AD dementia who also fulfilled the clinical criteria for pDLB had AD pathology with no LBD (6 of 8, 75%). Thus, the accuracy of identifying LBD significantly decreased in the setting of AD dementia diagnosis. There were cases in the LBD-AD group ($n = 7$) who were diagnosed with probable AD dementia and did not fulfill the clinical criteria for pDLB antemortem, even though they had intermediate- or high-likelihood LBD pathologically.

Pathologically, the LBD and LBD-AD groups were composed of cases with transitional or diffuse LBD, and the AD group had 4 cases without Lewy body pathology and 2 cases with amygdala-only Lewy body pathology, who were classified in the AD group because they had low-likelihood LBD with high AD pathology according to the 4th Consortium Criteria. As expected, the average Braak NFT stage and the Thal A β phase increased from the LBD to the LBD-AD and AD groups. Whereas none of the LBD cases had frequent NP and only 21% had moderate NP, 64% of the LBD cases had moderate to frequent DP. Thus, DP was far more abundant than NP in the LBD group. Three cases in the AD group and 3 cases in the LBD group had infarcts. Cerebral amyloid angiopathy (CAA) was observed in 2 cases in the LBD group and 1 case in the LBD-AD group.

PiB-PET findings in the pathologic groups

The voxel-based regional differences in PiB SUVR among the pathologic groups are displayed in figure 1. The AD group had greater PiB uptake in the entire cortex compared to the LBD group, while the uptake in the occipital cortex and the primary sensory and motor cortices was relatively spared in the LBD group compared to the LBD-AD group. The occipital cortex showed the greatest PiB uptake in the AD group compared to the LBD-AD group ($p < 0.05$) after correction for false discovery rate error.

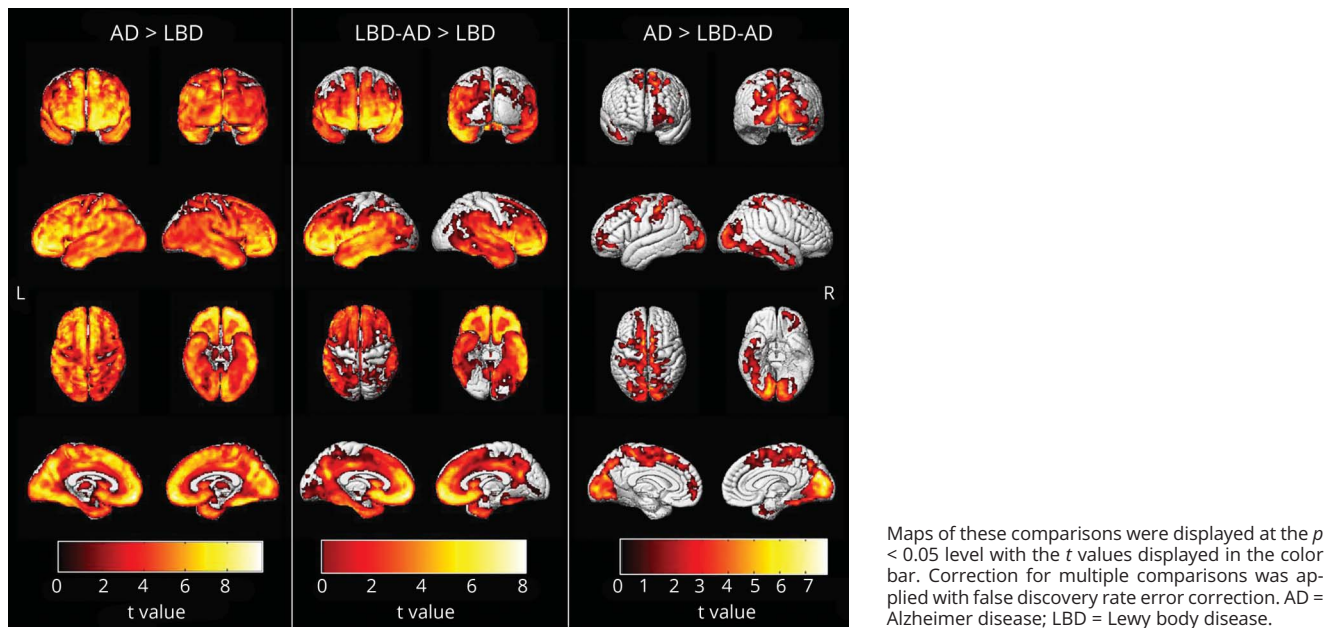
Figure 2A shows the differences in global cortical PiB uptake among the pathologic groups. In this cohort, global cortical PiB SUVR completely separated the AD and LBD pathologic groups from each other. The global cortical PiB SUVR distinguished cases with intermediate to high AD (i.e., LBD-AD and AD groups) from cases with LBD with low AD with 80% sensitivity, 86% specificity, and 93% accuracy (i.e., area under the receiver operating characteristic curve). The highest accuracy (93%) in distinguishing the 2 groups was at the cutoff PiB SUVR value of 1.88, which corresponds to the centiloid value of 56.74. Global cortical PiB SUVR correlated with the Thal A β phase in the entire cohort after adjustment for the time between imaging and death ($r = 0.75$, $p < 0.001$) (figure 2B).

PiB-PET findings and β -amyloid plaques in cases with LBD

Because one of our objectives was to determine the contribution of NP and DP to PiB-PET findings in cases with LBD, we included only cases with LBD and LBD-AD ($n = 33$) and excluded cases in the AD group ($n = 6$) from this analysis. Cases with no DP ($n = 4$) were combined with cases with sparse DP ($n = 2$); similarly, cases with no NP ($n = 2$) were combined with cases with sparse NP ($n = 12$) due to small numbers in either group.

PiB SUVR completely separated the LBD cases with no/sparse DP from those with frequent DP. There were 4 (25%) cases with no/sparse NP who had high PiB SUVR levels (>1.98), and these cases overlapped with the PiB SUVR of the cases with frequent NP. All 4 of these cases also had frequent DP. Another outlier was in the moderate NP group. This case had one of the lowest PiB SUVRs in the entire cohort and had moderate NP but no DP. Figure 3 shows the PiB SUVR values in cases with no/sparse to moderate to frequent NP and DP. In a multivariable model, we investigated the contribution of NP and DP levels to PiB SUVR and found that the PiB SUVR is driven primarily by the abundance of DP but not NP in the LBD and LBD-AD cases. The results of the multivariable model and the bar plot of average PiB SUVR when the NP and the DP categories are combined are presented in figure 4.

Figure 1 Voxel-based analysis comparing 11C-Pittsburgh compound B-PET standardized uptake value ratio in the LBD, mixed LBD-AD, and AD groups



Discussion

In a prospective cohort of patients with pDLB and autopsy-confirmed LBD cases who underwent antemortem PiB-PET examinations, global cortical PiB SUVr accurately distinguished cases with LBD from those with AD or mixed LBD and AD pathology, correlating with the Thal A β phase. Cortical PiB SUVr was lower in the occipital cortices in cases with LBD compared to mixed LBD and AD

pathology and in mixed LBD and AD pathology compared to cases with AD on voxel-based analysis. Furthermore, the severity of DP was the primary contributor to global cortical PiB SUVr in cases with LBD or mixed LBD and AD pathology.

In agreement with earlier autopsy studies of LBD, more than half of the cases we studied had coexisting AD-related pathology consisting of NPs and NFT-tau. All of the cases

Figure 2 Global cortical PiB SUVr in pathologic groups

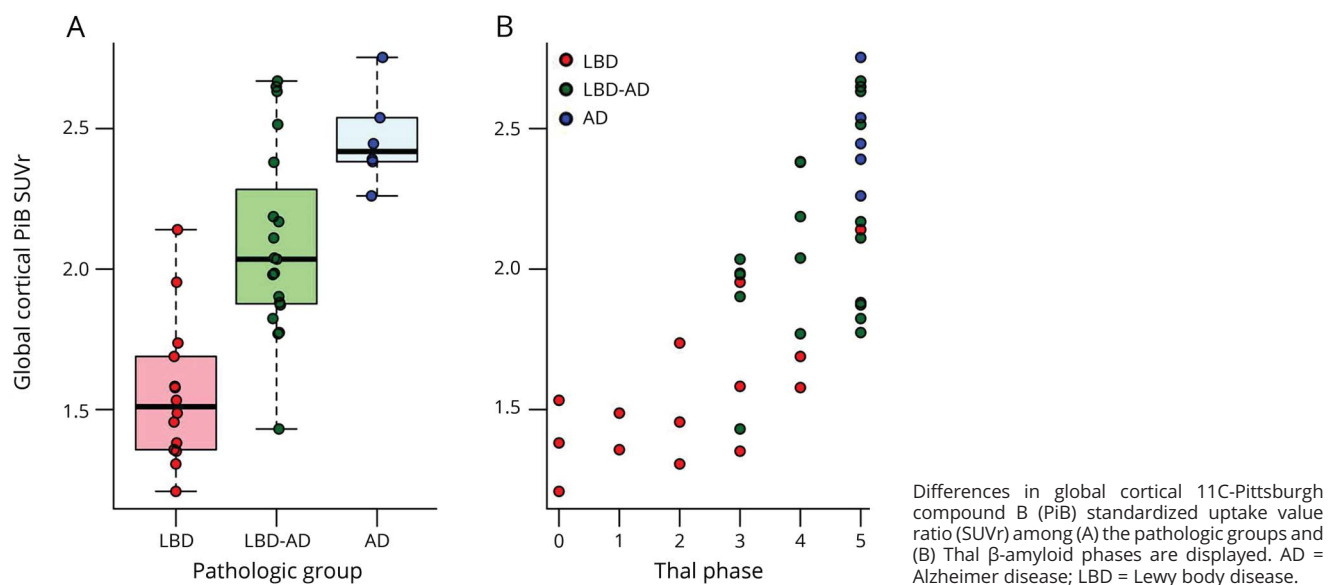
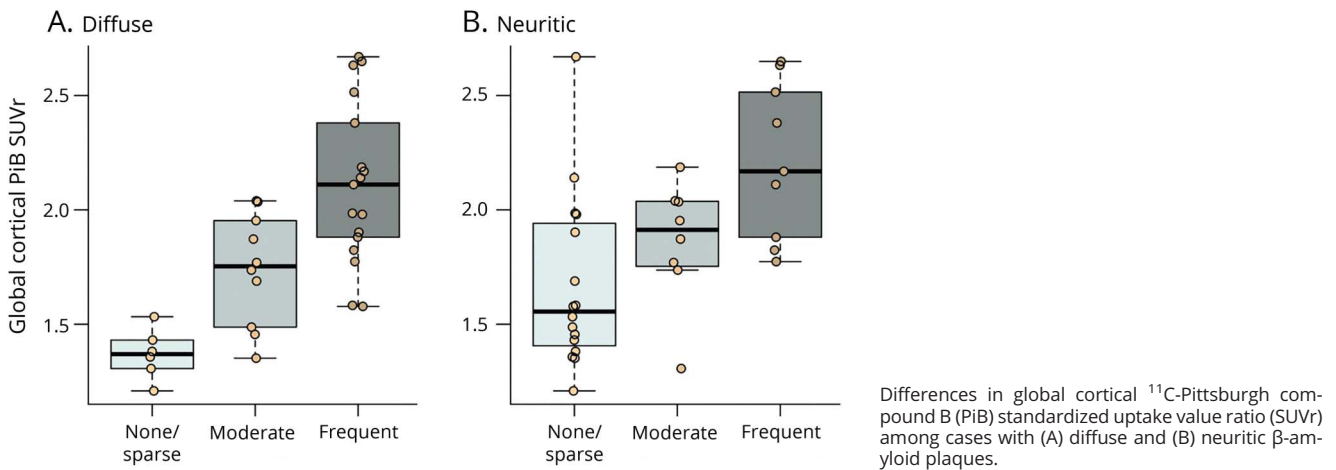


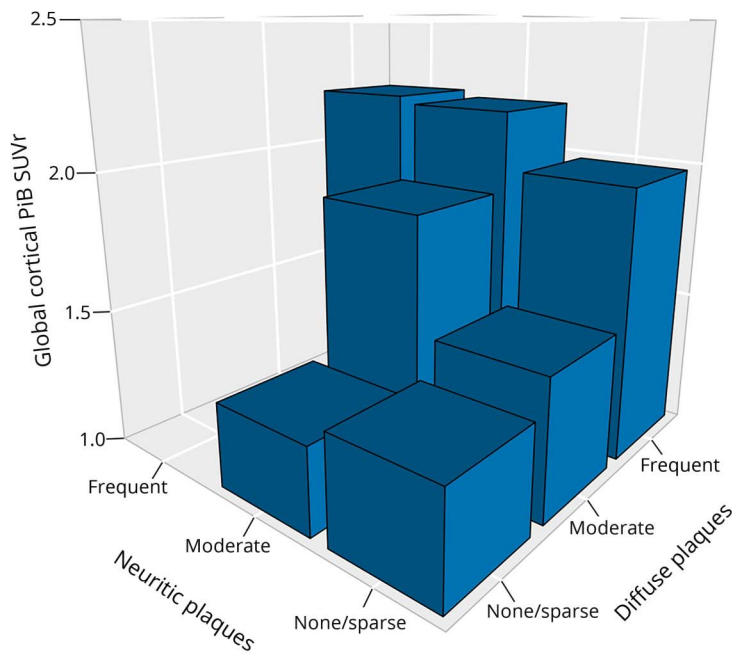
Figure 3 Global cortical PiB SUVr and β -amyloid plaques



in the LBD group were men, and approximately half of the cases in the LBD-AD group were women, suggesting that women with LBD are more likely to have mixed LBD and AD-related pathology. This sex difference in pathologic involvement requires further investigation.

As expected, cortical PiB SUVr was higher in the LBD-AD compared to the LBD group and in the AD compared to the LBD-AD group. Furthermore, cortical PiB SUVr completely separated the AD and LBD groups from each other. The topographic distribution of elevated cortical PiB SUVr

Figure 4 Contribution of neuritic and diffuse β -amyloid plaques to PiB SUVr in LBD



Multivariable model	Estimate	Standard error	p value
Intercept	0.738	0.445	0.11
Time from scan to death	-0.010	0.034	0.77
Neuritic amyloid- β plaques	0.287	0.330	0.39
Diffuse amyloid- β plaques	0.367	0.169	0.04
Neuritic*diffuse interaction	-0.049	0.115	0.67

The 3D bar graph shows the average ^{11}C -Pittsburgh compound B (PiB) standardized uptake value ratio (SUVr) when the neuritic and diffuse plaque categories are combined. This analysis was only done among the cases with Lewy body disease (LBD) and those with LBD-Alzheimer disease (n = 33).

followed a pattern that relatively spared the occipital cortices in the LBD compared to the LBD-AD group, and more significant involvement of the occipital cortices was observed in the AD compared to the LBD-AD group. This hierarchical pattern of relative sparing of the occipital cortices at lower levels of A β points out that those occipital lobe findings could contribute to the pathologic assessment and staging of A β pathology in cases with LBD. Elevated occipital cortex PiB SUVR has been associated with CAA.¹⁹ However, in this cohort, the only 2 cases with CAA were in the LBD group. Therefore, it is not possible to explain the relative sparing of the occipital cortex with the absence of CAA in cases with LBD. On the other hand, the relative sparing of the occipital cortex from A β pathology in cases with LBD may be influenced by pathophysiologic processes that characterize LBD.¹⁶ For example, patients with pDLB are characterized by hypometabolism in the occipital lobes³⁵ and degeneration in the temporal-occipital projections that are associated with visual hallucinations.³⁶ Thus, lower levels of A β pathology occur in a region that is functionally disrupted in patients with pDLB. This counterintuitive finding may be explained by mechanisms that lead to relative sparing of certain regions of the brain from the A β pathology. It was proposed that A β tends to deposit in regions showing continuous levels of heightened synaptic activation and plasticity.³⁷ In patients with LBD, synaptic plasticity is impaired due to Lewy neurites in the presynaptic terminals, and the occipital cortex is one of the regions affected. Moreover, to the extent that hypometabolism on PET is associated with synaptic integrity in LBD, the occipital cortex appears to be affected the most. Another and possibly related explanation may be the differences in A β plaque content (i.e., more abundant DP than NP) in patients with LBD. Whether relative sparing of occipital cortex from A β pathology is associated with higher levels of DP compared to NP in LBD needs to be investigated with quantitative pathologic assessment in samples from the occipital neocortex.

Elevated A β on PET scan is a common feature of pDLB, observed in up to 60% of patients with pDLB.^{4,5,23,38,39} Case reports demonstrated significant DP load contributing to elevated PiB SUVR, in some cases in the absence of additional AD-related pathology and the pathologic diagnosis of AD.^{6–8} In the current study, the primary determinant of PiB SUVR was the abundance of DP. In the absence of DP, NP was not a major contributor to PiB SUVR. Because frequent DP with low AD pathology is a distinct feature of LBD pathophysiology, higher PiB SUVR cutoff values may be needed for the classification of patients with pDLB who would qualify for the pathologic diagnosis of AD. In our cohort, a PiB SUVR value of 1.88, which corresponds to a centiloid value of 56.74, accurately distinguished the presence of intermediate to high AD according to the NIA-AA criteria. However, we note that a few cases with abundant DP and low AD pathology had higher PiB SUVR and a case with sparse DP, moderate NP, and intermediate AD had

lower PiB SUVR than this cutoff value. Whether the frequent DP and low AD pathology in LBD would evolve into AD is unknown. However, there is an association between the AV-1451 uptake and global cortical PiB SUVR in pDLB, suggesting that patients with pDLB with higher levels of A β also accumulate more tau pathology.¹

One limitation of this study that is common to all ante-mortem imaging and pathology correlation studies is that the time interval from the PET scan to death varied across individuals. Although no difference was found among the clinical groups and all analyses were adjusted for the length of this time interval, findings in individual patients should be interpreted with caution. Furthermore, one of the challenges in autopsy studies is the inclusion of cases with late-stage dementia. Hence, the subset of participants who were pathologically diagnosed as AD had very low MMSE scores.

With evolving A β -modifying therapies in patients within the AD spectrum, the inclusion of patients with pDLB, in whom A β influences disease progression and survival,^{1,2,40–43} is becoming a possibility in some trials targeting A β . Many patients with pDLB would be classified as A+ T– N– according to the NIA-AA research framework,⁴⁴ in part due to an abundance of DP. Whether modifying DP would influence disease progression in pDLB remains to be seen. However, with the use of a high cutoff for A β PET positivity, it is possible to accurately identify patients with pDLB who also have NP as part of intermediate to high AD pathology. This study provides the validation needed to identify patients with pDLB with AD-related pathology on the basis of A β PET.

Author contributions

K. Kantarci: design or conceptualization of the study, data collection, analysis and interpretation of the data, drafting the manuscript, study funding. V.J. Lowe: data collection, analysis or interpretation of the data, revising the manuscript. Q. Chen, S.A. Przybelski, T.G. Lesnick, C.G. Schwarz, M.L. Senjem, and J.L. Gunter: analysis or interpretation of the data, revising the manuscript. C.R. Jack, Jr., J. Graff-Radford, D.T. Jones, D.S. Knopman, N. Graff-Radford, T.J. Ferman, J.E. Parisi, D.W. Dickson, R.C. Petersen, B.F. Boeve, and M.E. Murray: data collection, analysis or interpretation of the data, revising the manuscript.

Study funding

This study was funded by the NIH (R01 AG040042, R01 AG11378, P50 AG16574, U01 AG06786, and C06 RR018898), the Foundation Dr. Corinne Schulerand, the Mangurian Foundation for Lewy Body Research, the Elsie and Marvin Dekelboum Family Foundation, and the Robert H. and Clarice Smith and Abigail Van Buren Alzheimer's Disease Research Program. The corresponding author had full access to all the data in the study and had final responsibility for the decision to submit for publication.

Disclosure

K. Kantarci serves on the Data Safety Monitoring Board for Takeda Global Research and Development Center, Inc; receives research support from Avid Radiopharmaceuticals and Eli Lilly; and receives funding from the NIH and Alzheimer's Drug Discovery Foundation. V. Lowe consults for Bayer Schering Pharma, Piramal Life Sciences, and Merck Research and receives research support from GE Healthcare, Siemens Molecular Imaging, AVID Radiopharmaceuticals, and the NIH (NIA, National Cancer Institute). Q. Chen, S. Przybelski, T. Lesnick, and C. Schwarz report no disclosures relevant to the manuscript. M. Senjem holds stock in Gilead Sciences, Inc, Inovio Pharmaceuticals, Medtronic, Oncothyreon, Inc, and PAREXEL International. J. Gunter reports no disclosures relevant to the manuscript. C. Jack provides consulting services for Eli Lilly. He is funded by the NIH and Alexander Family Alzheimer's Disease professorship of the Mayo Foundation. J. Graff-Radford and D. Jones report no disclosures relevant to the manuscript. D. Knopman served as deputy editor for *Neurology*; served on a Data Safety Monitoring Board for Lilly Pharmaceuticals; serves on a Data Safety Monitoring Board for Lundbeck Pharmaceuticals and for the Dominantly Inherited Alzheimer Network study; served as a consultant to TauRx Pharmaceuticals ending in November 2012; was an investigator in clinical trials sponsored by Baxter and Elan Pharmaceuticals in the past 2 years; is currently an investigator in a clinical trial sponsored by TauRx; and receives research support from the NIH (U01-HL096917, AG-037551). N. Graff-Radford, T. Ferman, J. Parisi, and D. Dickson report no disclosures relevant to the manuscript. R. Petersen consults for Roche, Inc, Merck, Inc, Genetech, Inc, Biogen, Inc, and Eli Lilly and Co, Pfizer, Elan Pharmaceuticals, Wyeth Pharmaceuticals, and GE Healthcare; receives royalties from the publication of *Mild Cognitive Impairment* (Oxford University Press, 2003); and receives research support from the NIH (UF1-AG32438, U19-AG24904, RF1-AG57547, U01-AG016976). B. Boeve has served as an investigator for clinical trials sponsored by GE Healthcare and Axovant; receives royalties from the publication of *Behavioral Neurology of Dementia* (Cambridge Medicine, 20179); serves on the Scientific Advisory Board of the Tau Consortium; and receives research support from the NIH (U01-AG045390, U54-NS092089, R01-AG041797, U01-NS100620, R01-AG38791), the Mayo Clinic Dorothy and Harry T. Mangurian Jr. Lewy Body Dementia Program, and the Little Family Foundation. M. Murray reports no disclosures relevant to the manuscript. Go to Neurology.org/N for full disclosures.

Publication history

Received by *Neurology* March 29, 2019. Accepted in final form August 7, 2019.

References

1. Ferman TJ, Aoki N, Crook JE, et al. The limbic and neocortical contribution of alpha-synuclein, tau, and amyloid beta to disease duration in dementia with Lewy bodies. *Alzheimers Dement* 2018;14:330–339.
2. Irwin DJ, Grossman M, Weintraub D, et al. Neuropathological and genetic correlates of survival and dementia onset in synucleinopathies: a retrospective analysis. *Lancet Neurol* 2017;16:55–65.

3. Walker L, McAleese KE, Thomas AJ, et al. Neuropathologically mixed Alzheimer's and Lewy body disease: burden of pathological protein aggregates differs between clinical phenotypes. *Acta Neuropathol* 2015;129:729–748.
4. Ossenkoppele R, Jansen WJ, Rabinovici GD, et al. Prevalence of amyloid PET positivity in dementia syndromes: a meta-analysis. *JAMA* 2015;313:1939–1949.
5. Gomperts SN, Rentz DM, Moran E, et al. Imaging amyloid deposition in Lewy body diseases. *Neurology* 2008;71:903–910.
6. Kantarci K, Yang C, Schneider JA, et al. Antemortem amyloid imaging and beta-amyloid pathology in a case with dementia with Lewy bodies. *Neurobiol Aging* 2012;33:878–885.
7. Backsai BJ, Frosch MP, Freeman SH, et al. Molecular imaging with Pittsburgh compound B confirmed at autopsy: a case report. *Arch Neurol* 2007;64:431–434.
8. Burack MA, Hartlein J, Flores HP, Taylor-Reinwald L, Perlmutter JS, Cairns NJ. In vivo amyloid imaging in autopsy-confirmed Parkinson disease with dementia. *Neurology* 2010;74:77–84.
9. Dugger BN, Clark CM, Serrano G, et al. Neuropathologic heterogeneity does not impair florbetapir-positron emission tomography postmortem correlates. *J Neuropathol Exp Neurol* 2014;73:72–80.
10. Seo SW, Ayakta N, Grinberg LT, et al. Regional correlations between [(11)C]PIB PET and post-mortem burden of amyloid-beta pathology in a diverse neuropathological cohort. *Neuroimage Clin* 2017;13:130–137.
11. Driscoll I, Troncoso JC, Rudow G, et al. Correspondence between in vivo (11)C-PIB-PET amyloid imaging and postmortem, region-matched assessment of plaques. *Acta Neuropathol* 2012;124:823–831.
12. Villeneuve S, Rabinovici GD, Cohn-Sheehy BI, et al. Existing Pittsburgh compound-B positron emission tomography thresholds are too high: statistical and pathological evaluation. *Brain* 2015;138:2020–2033.
13. Ikonomic MD, Buckley CJ, Heurling K, et al. Post-mortem histopathology underlying beta-amyloid PET imaging following flutemetamol F 18 injection. *Acta Neuropathol Commun* 2016;4:130.
14. Murray ME, Lowe VJ, Graff-Radford NR, et al. Clinicopathologic and 11C-Pittsburgh compound B implications of Thal amyloid phase across the Alzheimer's disease spectrum. *Brain* 2015;138:1370–1381.
15. Clark CM, Pontecorvo MJ, Beach TG, et al. Cerebral PET with florbetapir compared with neuropathology at autopsy for detection of neuritic amyloid-beta plaques: a prospective cohort study. *Lancet Neurol* 2012;11:669–678.
16. Dickson DW. Dementia with Lewy bodies: neuropathology. *J Geriatr Psychiatry Neurol* 2002;15:210–216.
17. Ikonomic MD, Klunk WE, Abrahamson EE, et al. Post-mortem correlates of in vivo PiB-PET amyloid imaging in a typical case of Alzheimer's disease. *Brain* 2008;131:1630–1645.
18. Lockhart A, Lamb JR, Osredkar T, et al. PIB is a non-specific imaging marker of amyloid-beta (Abeta) peptide-related cerebral amyloidosis. *Brain* 2007;130:2607–2615.
19. Johnson KA, Gregas M, Becker JA, et al. Imaging of amyloid burden and distribution in cerebral amyloid angiopathy. *Ann Neurol* 2007;62:229–234.
20. McKeith IG, Boeve BF, Dickson DW, et al. Diagnosis and management of dementia with Lewy bodies: fourth consensus report of the DLB Consortium. *Neurology* 2017;89:88–100.
21. Roberts RO, Geda YE, Knopman DS, et al. The Mayo Clinic Study of Aging: design and sampling, participation, baseline measures and sample characteristics. *Neuroepidemiology* 2008;30:58–69.
22. McKeith IG, Dickson DW, Lowe J, et al. Diagnosis and management of dementia with Lewy bodies: third report of the DLB Consortium. *Neurology* 2005;65:1863–1872.
23. Kantarci K, Lowe VJ, Boeve BF, et al. Multimodality imaging characteristics of dementia with Lewy bodies. *Neurobiol Aging* 2012;33:2091–2105.
24. Ferman TJ, Smith GE, Boeve BF, et al. DLB fluctuations: specific features that reliably differentiate DLB from AD and normal aging. *Neurology* 2004;62:181–187.
25. AASM. International Classification of Sleep Disorders–2: Diagnostic and Coding Manual. Chicago: American Academy of Sleep Medicine; 2005.
26. Mirra SS, Heyman A, McKeel D, et al. The Consortium to Establish a Registry for Alzheimer's Disease (CERAD), part II: standardization of the neuropathologic assessment of Alzheimer's disease. *Neurology* 1991;41:479–486.
27. Beach TG, White CL, Hamilton RL, et al. Evaluation of alpha-synuclein immunohistochemical methods used by invited experts. *Acta Neuropathol* 2008;116:277–288.
28. Hyman BT, Phelps CH, Beach TG, et al. National Institute on Aging-Alzheimer's Association guidelines for the neuropathologic assessment of Alzheimer's disease. *Alzheimers Dement* 2012;8:1–13.
29. Montine TJ, Phelps CH, Beach TG, et al. National Institute on Aging-Alzheimer's Association guidelines for the neuropathologic assessment of Alzheimer's disease: a practical approach. *Acta Neuropathol* 2012;123:1–11.
30. Thal DR, Rub U, Orantes M, Braak H. Phases of A beta-deposition in the human brain and its relevance for the development of AD. *Neurology* 2002;58:1791–1800.
31. Besser LM, Kukull WA, Teylan MA, et al. The revised National Alzheimer's Coordinating Center's Neuropathology form: available data and new analyses. *J Neuropathol Exp Neurol* 2018;77:717–726.
32. Braak H, Braak E. Neuropathological staging of Alzheimer-related changes. *Acta Neuropathol* 1991;82:239–259.
33. Schwarz CG, Gunter JL, Ward C, et al. The Mayo Clinic Adult Lifespan Template: better quantification across the lifespan. *Alzheimers Dement* 2017;13:P792.
34. Jack CR Jr, Lowe VJ, Senjem ML, et al. 11C PiB and structural MRI provide complementary information in imaging of Alzheimer's disease and amnesic mild cognitive impairment. *Brain* 2008;131:665–680.

35. Ishii K, Imamura T, Sasaki M, et al. Regional cerebral glucose metabolism in dementia with Lewy bodies and Alzheimer's disease. *Neurology* 1998;51:125–130.
36. Kantarci K, Avula R, Senjem ML, et al. Dementia with Lewy bodies and Alzheimer disease: neurodegenerative patterns characterized by DTI. *Neurology* 2010;74:1814–1821.
37. Jagust WJ, Mormino EC. Lifespan brain activity, beta-amyloid, and Alzheimer's disease. *Trends Cogn Sci* 2011;15:520–526.
38. Maetzler W, Liepelt I, Reimold M, et al. Cortical PIB binding in Lewy body disease is associated with Alzheimer-like characteristics. *Neurobiol Dis* 2009;34:107–112.
39. Edison P, Rowe CC, Rinne JO, et al. Amyloid load in Parkinson's disease dementia and Lewy body dementia measured with [¹¹C]PIB positron emission tomography. *J Neurol Neurosurg Psychiatry* 2008;79:1331–1338.
40. Compta Y, Parkkinen L, O'Sullivan SS, et al. Lewy- and Alzheimer-type pathologies in Parkinson's disease dementia: which is more important? *Brain* 2011;134:1493–1505.
41. Graff-Radford J, Lesnick TG, Boeve BF, et al. Predicting survival in dementia with Lewy bodies with hippocampal volumetry. *Mov Disord* 2016;31:989–994.
42. Jellinger KA, Seppi K, Wenning GK, Poewe W. Impact of coexistent Alzheimer pathology on the natural history of Parkinson's disease. *J Neural Transm (Vienna)* 2002;109:329–339.
43. Sarro L, Senjem ML, Lundt ES, et al. Amyloid-beta deposition and regional grey matter atrophy rates in dementia with Lewy bodies. *Brain* 2016;139:2740–2750.
44. Jack CR Jr, Bennett DA, Blennow K, et al. NIA-AA research framework: toward a biological definition of Alzheimer's disease. *Alzheimers Dement* 2018;14:535–562.